Journal for ImmunoTherapy of Cancer

Pattern recognition receptor agonists in pathogen vaccines mediate antitumor T-cell cross-priming

Mark Aleynick ,[1,2,3] Judit Svensson-Arvelund,[2,3] Gvantsa Pantsulaia,[2,3] Kristy Kim,[2,3] Samuel A Rose,[1,2] Ranjan Upadhyay,[1,2,3] Michael Yellin,[4] Henry Marsh,[4] Daniel Oreper,[5] Suchit Jhunjhunwala,[5] Christine Carine Moussion ,[5] Miriam Merad,[2] Brian D Brown,[2] Joshua D Brody[2,3]

To cite: Aleynick M, Svensson-Arvelund J, Pantsulaia G, *et al*. Pattern recognition receptor agonists in pathogen vaccines mediate antitumor T-cell cross-priming. *Journal for ImmunoTherapy of Cancer* 2023;**11**:e007198. doi:10.1136/jitc-2023-007198

► Additional supplemental material is published online only. To view, please visit the journal online (http://dx.doi.org/10.1136/jitc-2023-007198).

Accepted 21 June 2023

[1]Graduate School of Biomedical Sciences, Icahn School of Medicine at Mount Sinai, New York, New York, USA
[2]Marc and Jennifer Lipschultz Precision Immunology Institute, Icahn School of Medicine at Mount Sinai, New York, New York, USA
[3]Hematology and Medical Oncology, Icahn School of Medicine at Mount Sinai, New York, New York, USA
[4]Celldex Therapeutics Inc, Hampton, New Jersey, USA
[5]Genentech Inc, South San Francisco, California, USA

Correspondence to
Joshua D Brody;
joshua.brody@mssm.edu

ABSTRACT

Background Cancer immunotherapies are generally effective in patients whose tumors contain a priori primed T-cells reactive to tumor antigens (TA). One approach to prime TA-reactive T-cells is to administer immunostimulatory molecules, cells, or pathogens directly to the tumor site, that is, in situ vaccination (ISV). We recently described an ISV using Flt3L to expand and recruit dendritic cells (DC), radiotherapy to load DC with TA, and pattern recognition receptor agonists (PRRa) to activate TA-loaded DC. While ISV trials using *synthetic* PRRa have yielded systemic tumor regressions, the optimal method to activate DCs is unknown.

Methods To discover optimal DC activators and increase access to clinical grade reagents, we assessed whether viral or bacterial components found in common pathogen vaccines are an effective source of *natural PRRa* (*naPRRa*). Using deep profiling (155-metric) of naPRRa immunomodulatory effects and gene editing of specific PRR, we defined specific signatures and molecular mechanisms by which naPRRa potentiate T-cell priming.

Results We observed that vaccine naPRRa can be even more potent in activating Flt3L-expanded murine and human DCs than synthetic PRRa, promoting cross-priming of TA-reactive T-cells. We developed a mechanistically diverse naPRRa combination (BCG, PedvaxHIB, Rabies) and noted more potent T-cell cross-priming than with any single naPRRa. The naPRRa triplet—as part of Flt3L-primed ISV—induced greater intratumoral CD8 T-cell infiltration, T-cells reactive to a newly defined tumorous neoantigen, durable tumor regressions.

Conclusions This work provides rationale for the translation of pathogen vaccines as FDA-approved clinical-grade DC activators which could be exploited as immune-stimulants for early phase trials.

WHAT IS ALREADY KNOWN ON THIS TOPIC

⇒ Priming tumor-specific T-cells through vaccination can be an effective method to drive a robust anti-tumor immune response. Strategies such as in situ vaccination (ISV) rely on antigen presenting cells, including dendritic cells (DCs), which are loaded with tumor antigens and activated using pattern recognition receptor agonists (PRRa).

WHAT THIS STUDY ADDS

⇒ Although vaccination using synthetic PRRa have yielded tumor regressions, the optimal method to activate DCs is unknown, and the limited availability of demonstrably safe clinical-grade PRRa hinders clinical progress. To address these challenges, we investigated whether common pathogen vaccines (M-M-R, Typhim Vi, etc) could serve as *natural* PRRa (naPRRa) to mediate DC activation. We found that several naPRRa potently activate DCs and enhance tumor antigen cross-presentation vs synthetic PRRa. When used as part of a Flt3L-primed ISV, we demonstrate that naPRRa promote intratumoral CD8 T-cell infiltration, prime tumor-neoantigen-specific T-cells, and induce durable tumor regressions.

HOW THIS STUDY MIGHT AFFECT RESEARCH, PRACTICE OR POLICY

⇒ Our study demonstrates that pathogen vaccines are effective DC activators and provides rationale for their translation as clinical-grade reagents, available for immediate use in early phase trials.

INTRODUCTION

Most cancer immunotherapies depend on the induction of primed CD8 T-cells recognizing tumor antigens (TA) presented on major histocompatability complex I (MHC-I) ('signal 1'). TA may be *directly* presented by tumor cells, providing signal 1 in isolation, which can be more tolerogenic than immunogenic. Alternatively, TA can be *cross*-presented by antigen presenting cells (APC), providing signal 1 in the context of signal 2 (eg, CD80) and signal 3 (eg, IL-12). Immunotherapies, including checkpoint blockade, T-cell transfer, and vaccines, fail completely in the absence of cross-presenting dendritic cells (DC).[1–5] Conversely, *increasing* intratumoral DC potentiates cross-presentation to anti-tumor T-cells and clinical responses.[6] Optimal antitumor T-cell responses require that DC are mobilized, loaded with TA, and activated.

Critical questions include how best to load DC with TA and how best to activate TA-loaded DC. One approach to DC loading is to define neoantigen TA by individualized tumor exome and RNA sequencing, in silico prediction, peptide synthesis, and administration. Such neoantigen vaccines have induced neoantigen-reactive T-cells in early trials; however, this approach is time and resource intensive. Time to treatment is an important limitation; months of vaccine preparation may preclude this approach for aggressive tumors. Similarly, resource intensity is an important limitation, as cancer immunotherapy has not equally benefited all patients; cohort studies of more than 50 000 patients demonstrate that underinsured status and socioeconomic metrics correlate with access to immunotherapies.[7 8]

An alternative, less time and resource-intensive approach, is to load DC *at the site of* a patient's tumor. This 'off-the-shelf' in situ vaccination (ISV)[6 9] approach can *mobilize*, *load*, and *activate* DC intratumorally; activated DC then cross-prime tumor-reactive CD8 T-cells. Previously, we described an ISV comprising Flt3-ligand (Flt3L) to *mobilize* DC, radiotherapy (XRT) to release TA and *load* DC, and intratumoral (i.t.) administration of a pattern-recognition-receptor agonist (PRRa) to *activate* antigen-loaded DC.[6] While trials of ISV using *synthetic* PRRa have yielded tumor regressions,[6 10–13] the optimal approach to activate DC is unknown, and the limited availability of safe, clinical grade PRRa impedes clinical progress. Because synthetic PRRa are designed to mimic pathogen associated molecular patterns, common pathogen vaccines (eg, Typhim Vi, M-M-R, BCG) may be a robust source of *natural* PRRa (naPRRa).[14]

Although there are some examples of naPRRa-mediated antitumor immunity,[15 16] little is known regarding using pathogen vaccines to activate DC for cancer vaccination.[17] An exception is BCG, which induces inflammation and local tumor regressions in early stage bladder cancer, though the molecular and cellular mechanisms are poorly understood.[18] Here, we present the most extensive immune profiling of 19 commonly available pathogen vaccines performed to date. Using murine and patient-derived DC, we demonstrate that pathogen vaccines contain naPRRa which can be more potent than synthetic PRRa in activating DC and cross-priming cytotoxic CD8 T-cells. Using knockout mouse-derived and CRISPR-cas9 gene edited APC, we define specific molecular mechanisms of naPRRa in pathogen vaccines. Combining mechanistically distinct naPRRa, we create a rational triplet combination which induces greater-than-additive T-cell cross-priming and—as part of ISV—induces durable tumor regressions. We identified novel tumor neoantigen candidates and demonstrate that naPRRa-ISV induces neoantigen-reactive T-cells, accomplishing a similar result to personalized neoantigen vaccines with an off-the-shelf approach.

RESULTS

Pathogen vaccines function as naPRRa to activate patient and murine DCs

As noted, there is a major interest in developing effective approaches for ISV, which would overcome the need for sequencing patient tumors to create patient-specific antigen vaccines. We previously demonstrated that *synthetic* PRRa potentiate cross-presentation and systemic tumor regressions in patients and murine models as part of a Flt3L-mobilized ISV.[6] Therefore, we hypothesized that Flt3L-mobilized APC subsets may also be responsive to naPRRa present in pathogen vaccines and assessed this using peripheral blood mononuclear cells (PBMC) from Flt3L-treated patients. Employing 22-metric spectral flow cytometry, we identified nine distinct immune cell populations, including four DC subsets, per viSNE clustering (figure 1A, left panel). Pathogen vaccines (eg, PedvaxHIB, BCG, Typhim) induced activation of innate immune cell subsets, including monocytes, plasmacytoid DC (pDC) and conventional DC (cDC) subsets, that is, $CD141^+$ DC1, $CD1c^+$ DC2, and double-negative DC (DN DC), upregulating costimulatory (CD40, CD80, CD86) and inhibitory (PD-L1) molecules (figure 1A, middle panel, online supplemental figure S1a). Activation was most dynamic in cDC subsets (figure 1A, middle and right panels) and significant versus no PRRa for 8 of 19 vaccines tested.

Next, we examined naPRRa effects on murine APCs using splenocytes from Flt3L-treated mice. Using 27-metric spectral flow cytometry, we again identified nine distinct cell populations (figure 1B, left panel) and assessed activation status following exposure to the 19 vaccines. The cDC cluster containing $XCR1^+$ DC1, $CD11b^+$ DC2, and DN DC responded dynamically to naPRRa, expressing greater levels of costimulatory markers both at baseline and after naPRRa activation as compared with other APC subsets (figure 1B, middle panel, figure 1C, online supplemental figure S1b). DC activation was significant versus no PRRa for 10 of the 19 vaccines (6 overlapping with human DC) and notably, several (BCG, PedvaxHIB, Rabies) were more potent ($p<0.05$) DC activators than the synthetic PRRa PolyIC (figure 1B, right panel).

As previously, DC were enriched in Flt3L-primed mice (figure 1D, online supplemental figure S1c).[6] Again, naPRRa potently activated DC, even more so than PolyIC ($p<0.05$), both in Flt3L-primed and untreated mice (online supplemental figure S1d). All DC subsets upregulated costimulatory molecules with some naPRRa (online supplemental figure S1e). pDC were activated by several naPRRa, most potently by BCG, Rabies vaccine, and PedvaxHIB (online supplemental figure S1e). Interestingly, Rabies, Measles-Mumps-Rubella (MMR), and varicella zoster vaccines (VZV) potently activated macrophages, despite lesser effects on cDC (online supplemental figure S1b). These data suggest that, rather than one 'best' naPRRa, individual APC subsets are differentially activated by distinct naPRRa. Though DC may be critical for antitumor immunity, the heterogeneity of tumor immune cell infiltrates[19 20] suggests that targeting *multiple* APC subsets might optimally modulate the suppressive tumor microenvironment (TME).

In addition to costimulatory molecules (signal 2), cytokines produced by APCs are critical in T-cell priming

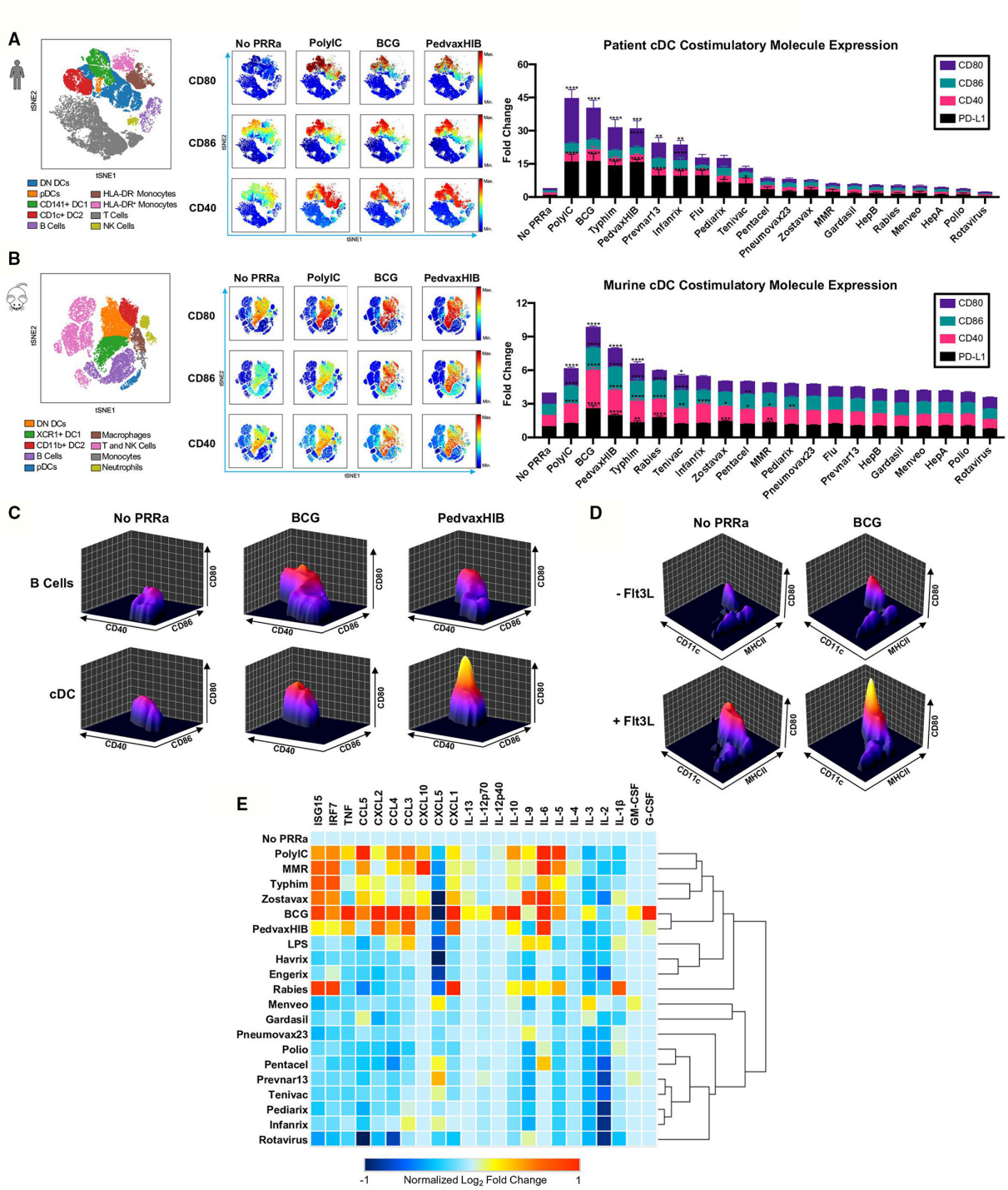

Figure 1 Pathogen vaccines can function as naPRRa to activate both murine and human DCs. Patient PBMCs or murine splenocytes were activated with naPRRa and analyzed by spectral flow cytometry. (A) Immune cell populations in PBMCs from two patients visualized by viSNE (*left*). Representative viSNE plots show indicated activation marker expression (*middle*), and bar graph (*right*) quantifies mean fluorescence intensity (MFI) fold changes of indicated activation marker expression in the aggregate cDC cluster (DN DC, DC1, DC2). Statistical significance was calculated against No PRRa condition by two-way ANOVA with Dunnett's multiple comparison test. (B) Representative viSNE plots showing murine splenocyte subsets (*left*) indicated activation marker expression (*middle*) and bar graph (*right*) of mean MFI fold changes of activation marker expression in the aggregate cDC cluster (DN DC, DC1, DC2). Statistical significance was calculated comparing against No PRRa by two-way ANOVA with Dunnett's multiple comparison test; data from three independent experiments. (C) Representative cytomountain plots comparing cDC and B cell costimulatory marker expression in response to naPRRa. (D) Representative cytomountain plots depicting activation of in vivo Flt3L-generated DCs by the naPRRa BCG. (E) Heatmap summarizing CD11c$^+$ DC cytokine production and type I interferon response after naPRRa stimulation, as measured by multiplex bead assay and qPCR, respectively. DC cytokines that did not change from baseline on stimulation are not shown. ANOVA, analysis of variance; DC, dendritic cells; DN, double-negative; PRRa, pattern recognition receptor agonists.

(signal 3). To assess this, we treated Flt3L-primed splenocytes with naPPRa, measuring cytokines and type I IFN inducible transcripts by Luminex and qPCR, respectively. We observed dynamic cytokine production upon naPRRa treatment (figure 1E), even from naPRRa that induced no cDC phenotypic activation. For example, MMR did not induce CD40/80/86, but promoted a type I interferon response and IL-6 production (~9.6-fold increase). Only the Hepatitis A (Havrix) vaccine appeared inert, suggesting that most pathogen vaccines do contain naPRRa. Some naPRRa appeared more potent than synthetic PRRa in pathways critical for T-cell cytotoxicity,[2 21] for example, IL-12p70 was induced by BCG but not by PolyIC. Although BCG and PedvaxHIB were the most potent cytokine-inducers, there was no single best inducer of all cytokines. Rabies vaccine uniquely induced IL-1β, a potent activator of macrophages, whereas MMR uniquely induced CXCL10, a critical chemokine in recruiting intratumoral natural killer (NK) and CD8 T-cells.[4 22–25] Several naPRRa induced the CCR5 ligands CCL3/CCL4/CCL5 which recruit disparate antitumoral effector cells to the TME.[26 27] Distinct naPRRa induced type I interferon signaling, which promotes DC function and T-cell priming against TA.[28 29] For example, Rabies and BCG induced sevenfold and threefold more IRF7, and sevenfold more ISG15[30 31] than PolyIC (figure 1E). The distinct cytokine profiles induced by individual naPRRa suggest that rational naPRRa combinations may yield non-obvious, greater-than-additive immunomodulation.

naPRRa-activated DC prime patient CD8 and CD4 T-cells

To assess the capacity of patient DCs to activate T-cells, we developed an assay using staphylococcus enterotoxin B (SEB) (figure 2A), cross-linking MHC on APCs with the T-cell receptor (TCR) on T-cells, as a surrogate for antigen-specific MHC/TCR interactions.[32] Herein, SEB-mediated T-cell activation is potentiated by APC costimulatory signals including CD80 and CD86.[32 33] We cultured PBMCs from Flt3L-treated patients with SEB and confirmed that SEB promotes cytokine production in both CD4 and CD8 T-cells (online supplemental figure S2a).

We observed that 10 of the 19 naPRRa enhanced CD8 or CD4 T-cell priming over the no PRRa condition, evidenced by increased cytokine production (figure 2B), including 3 naPRRa that did not induce phenotypic cDC activation (Zostavax, Pneumovax23, and Pentacel). Of these 10, several were more potent than PolyIC (figure 2B). Notably, Prevnar13 and Pneumovax23 potentiated patient T-cell priming despite lack of effects in murine DCs (figure 1B), suggesting species-specific effects, possibly due to differences in PRR repertoire among immune cell subsets.[34] Overall, these data demonstrate that naPRRa can enhance APC-mediated priming of patient T-cells, and that several are more effective than the commonly used synthetic PRRa PolyIC.

naPRRa-activated DC cross-prime antigen-specific CD8 T-cells

Our observations of DC activation suggest that naPRRa may potentiate antigen cross-presentation. To assess DC cross-presentation, splenocytes from Flt3L-treated mice were pulsed with ovalbumin (Ova), naPRRa-activated, and cocultured with OT-1 CD8 T-cells. Minimal cross-priming of OT-1 cells occurred without PRRa, per IFNγ production (online supplemental figure S3a), proliferation (online supplemental figure S3b), and CD69 expression (online supplemental figure S3c) versus no-antigen controls, indicating cross-presentation of $Ova^{257\text{-}264}$ SIINFEKL peptide. However, DCs stimulated with five of the naPRRa markedly potentiated OT-1 cross-priming, with several as or *more* effective than PolyIC; PedvaxHIB induced twice as much IFNγ production as PolyIC ($p<0.0001$) (online supplemental figure S3a). Different naPRRa were superior in potentiating different cross-priming metrics, suggesting that assessing more metrics might better depict naPRRa immunomodulatory effects.

naPRRa-activated DCs cross-prime cytotoxic CD8 T-cells against TA

Whereas soluble antigens, for example, Ova are captured by DCs through macropinocytosis,[35] dying cancer cells are instead cleared primarily through phagocytic receptors.[36–38] To study this more relevant biology, we developed a system to model DC uptake of tumor cell antigen. Using CRISPR-Cas9 gene editing, we generated GFP-A20 lymphoma cells lacking beta 2 microglobulin (B2m). Co-culturing irradiated (irr) $B2m^{-/-}$ GFP-A20, DC, and anti-GFP CD8 T-cells,[39] we assessed DC capacity to cross-present tumor derived GFP (figure 2C), as $B2m^{-/-}$ GFP-A20 cannot directly present antigen. DCs cocultured with irr-$B2m^{-/-}$A20 (*lacking* GFP) fail to induce anti-GFP CD8 T-cell proliferation, regardless of PRRa activation (online supplemental figure S4a). When cocultured with irr-$B2m^{-/-}$*GFP*-A20 however, DCs induce moderate, antigen-restricted, anti-GFP T-cell proliferation, which is potentiated by DC activation with the synthetic PRRa PolyIC, and significantly more so with BCG-activated DCs.

We observed that naPRRa-activated DC cross-prime anti-GFP CD8 T-cells to induce IFNγ and TNF (figure 2D), key mediators of the T-cell antitumor response. DCs activated with BCG induced a more potent TNF response than synthetic PRRa PolyIC ($p=0.0002$) and DC activation with several naPRRa candidates, including BCG, Typhim, Rabies, MMR, and PedvaxHIB, cross primed anti-GFP CD8 T-cells to proliferate to similar or greater levels than that seen with synthetic PRRa PolyIC (figure 2E). Notably, ~60% of CD8 T-cells in JEDI mice are GFP-specific,[39] therefore *most* Ag-specific T-cells are cross-primed by naPRRa-activated DC.

To assess cytotoxicity of anti-GFP CD8 T-cells cross-primed by naPRRa-activated DC, the former were cocultured with 50:50 mixtures of *B2m*-expressing GFP-A20 (target) cells and mCherry-A20 cells (figure 2C) using the resulting GFP:mCherry ratio as cytotoxicity

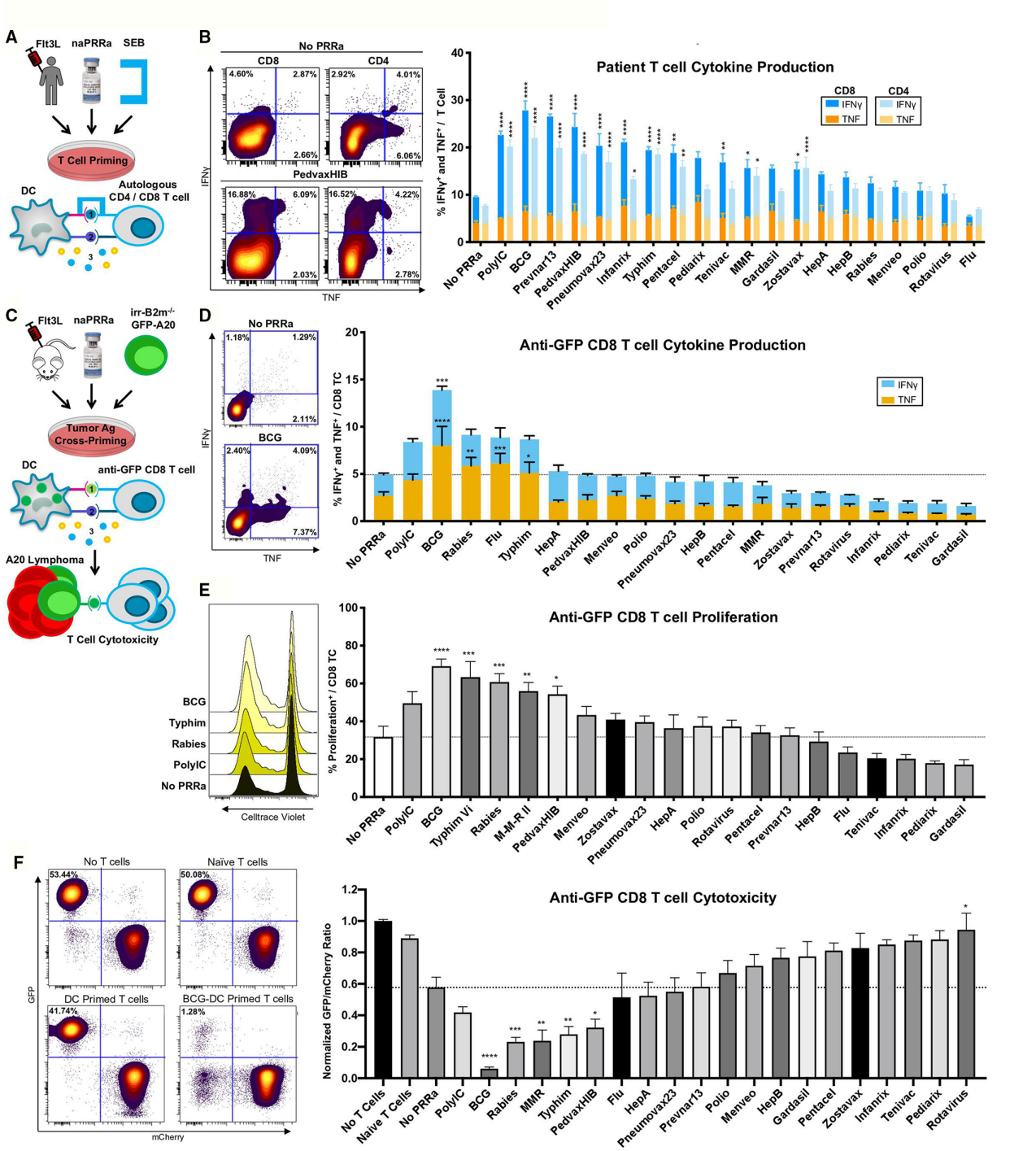

Figure 2 naPRRa-activated DC effectively prime and cross-prime T-cells. (A) Schema of SEB assay. PBMCs from four Flt3L-treated patients were treated with naPRRa and SEB. T-cell activation was measured by flow cytometry. (B) Representative scatter plots and bar graph summarizing CD8 and CD4 T-cell IFN-γ and TNF production in response to SEB+naPRRa. Statistical significance was calculated against 'No PRRa' condition by two-way ANOVA with Tukey's multiple comparisons test. (C) Schema of the cross-presentation assay. DCs were cocultured with XRT B2m$^{-/-}$GFP-A20, activated with naPRRa, and used to cross-prime anti-GFP CD8 T-cells. CD8 T-cell activation was measured as (D) production of IFN-γ and TNF and (E) proliferation. (F) After 96 hours of cross-priming, GFP/mCherry-A20 cells were added to assess anti-GFP CD8 T-cell cytotoxicity. Representative scatter plots and bar graph showing normalized GFP/mCherry ratio after 24 hours coculture with anti-GFP CD8 T-cells. Decreasing ratio indicates loss of GFP-A20, mediated by cytotoxic anti-GFP CD8 T-cells. Statistical significance was calculated by two-way ANOVA (D) or one-way ANOVA (E,F) with Dunnett's multiple comparison test, comparing to the 'No PRRa' condition. ANOVA, analysis of variance; DC, dendritic cells; PRRa, pattern recognition receptor agonists; SEB, staphylococcus enterotoxin B.

metric, as described.[6 40 41] Naïve anti-GFP CD8 T-cells displayed minimal cytotoxicity; however, cross-primed T-cells reduced GFP:mCherry ratios from ~1 to ~0.6 (figure 2F). Activating DCs with PRRa further potentiates cross-primed T-cell cytotoxicity. T-cells cross-primed by BCG-activated DC reduced GFP:mCherry ratios to 0.06, significantly lower than PolyIC (p=0.0005). Interestingly, some naPRRa which induced T-cell cytokines (eg, influenza) failed to induce cytotoxicity; conversely other naPRRa which induce cytotoxicity (eg, MMR) did not induce cytokines. These results demonstrate that naPRRa can activate DCs to cross-present tumor-derived antigen to CD8 T-cells, but also suggest that no *single* metric predicts optimal naPRRa-potentiation of cross-priming.

Immune-metric dimensionality reduction reveals unique activation profiles of naPRRa

Functional naPRRa show unique profiles: some naPRRa induce highly activated cDC phenotypes (eg, BCG, PedvaxHIB), while others induce type I IFN stimulated genes (eg, Rabies). Differences in naPRRa profiles suggest that individual naPRRa may act via distinct mechanisms. The DC-assays (figure 1) are more straightforward than the multicell culture T-cell assays (figure 2) and more feasible for additional human studies, whereby autologous T-cell cross-priming is difficult to assess. If simpler DC assays *could* predict results of T-cell cross-priming, this would improve understanding of DC-T-cell interactions and facilitate clinical translation.

Compiling datasets generated in figure 1, we identified 155 unique parameters, including costimulatory marker expression of multiple immune cell subsets, cytokine production, and naPRRa-induced type I interferon response. Dimensionality reduction by principal component analysis (PCA) was performed on this 155-metric dataset (figure 3A and online supplemental figure S5a,b). naPRRa that failed to induce T-cell cytotoxicity mainly cluster together (red ellipse region), segregating from naPRRa that promoted T-cell cytotoxicity (blue ellipse). Interestingly, effective naPRRa seem to additionally segregate from each other. Rabies and MMR naPRRa, viral vaccines that potently induce T-cell cytotoxicity, segregate by PC2, while BCG strongly segregates by PC1. This suggests that effective naPRRa may differ mechanistically, activating DC by distinct pathways.

naPRRa function through TRIF and MyD88

To assess whether naPRRa activate different PRRs, we first assessed PRRa-mediated DC activation in splenocytes from Flt3L-treated TRIF$^{-/-}$ and MyD88$^{-/-}$ mice. We observed that several naPRRa function through TRIF- and/or MyD88-mediated mechanisms (figure 3B). Activation with Rabies, MMR, and Zostavax naPRRa is diminished in MyD88$^{-/-}$ DCs whereas activation with BCG, PedvaxHIB, and Typhim naPRRa is diminished in both TRIF$^{-/-}$ and MyD88$^{-/-}$ DCs. These results indicate that several vaccine naPRRa require TRIF—suggesting toll-like receptor (TLR) 3 or TLR4 signaling—and/or MyD88—suggesting other TLR signaling—to activate DC. Some naPRRa (eg, MMR) maintain partial signaling despite absence of Myd88 or TRIF suggesting alternate signaling mechanisms.

TLR$^{-/-}$ RAW macrophages reveal specific TLR mechanism of several naPRRa

Identifying naPRRa with non-overlapping mechanisms may yield greater-than-additive effects when combined, generating optimal DC activation. Specific PRR utilization by most approved vaccines is unknown.[14] We gene-edited individual TLR from RAW macrophages, generating TLR$^{-/-}$ cell lines for TLR2$^{-/-}$, TLR4$^{-/-}$, TLR7$^{-/-}$, and TLR9$^{-/-}$ (online supplemental figure S5c) and evaluated naPRRa activation of TLR$^{-/-}$ RAW cells (figure 3C). TLR2$^{-/-}$ macrophages were unable to respond to BCG (figure 3D), indicating BCG predominantly functions through TLR2 here. Typhim showed complete loss of activity in TLR4$^{-/-}$ macrophages, similar to LPS (figure 3E). PedvaxHIB-effects were diminished in TLR4$^{-/-}$ cells. None of the naPRRa appeared to signal through TLR7 or TLR9 (online supplemental figure S5d,e).

For the TLR identifiable naPRRa—BCG, Typhim, and PedvaxHIB—we assessed whether naPRRa APC-activation was necessary for T-cell priming and cross-priming. WT or TLR$^{-/-}$ RAW cells were cocultured with GFP-peptide, activated with PRRa, and cultured with anti-GFP CD8 T-cells (figure 3C). BCG-activated TLR2$^{-/-}$ macrophages lost ability to prime T-cells (figure 3F). Similar results were observed with Typhim and TLR4$^{-/-}$ RAW cells. Interestingly, while macrophage phenotypic activation by PedvaxHIB was only reduced in the TLR4$^{-/-}$ setting, PedvaxHIB lost T-cell priming using both TLR4$^{-/-}$ *and* TLR2$^{-/-}$ cells, suggesting greater discovery power with these T-cell assays. Further, *cross*-presentation of B2m$^{-/-}$ GFP-A20-derived GFP by BCG-activated macrophages was TLR2-dependent and by Typhim-activated macrophages was TLR4-dependent (figure 3G). As above, PedvaxHIB-potentiated cross-priming was both TLR2-dependent and TLR4-dependent. These results indicate that individual naPRRa promote APC activation through distinct TLR, yielding differential priming and cross-priming of CD8 T-cells.

Feature selection and dimensionality reduction identify a predictive model for naPRRa efficacy

Distinct naPRRa mechanisms led us to look for common features between effective naPRRa. Starting with our 155 phenotypic-marker dataset, feature selection determined those that correlate with naPRRa killing score by Spearman correlation (adjusted p<0.01). Forty-three phenotypic markers that correlated with DC priming of cytotoxic T-cells were identified (online supplemental figure S6a). PCA was performed on these 43 markers to reduce noise and generate more robust clustering. In this simplified PCA, effective naPRRa clearly segregate from ineffective naPRRa by PC1, with Zostavax as a single (PC1^{high} but Killing Score^{low}) outlier (figure 4A

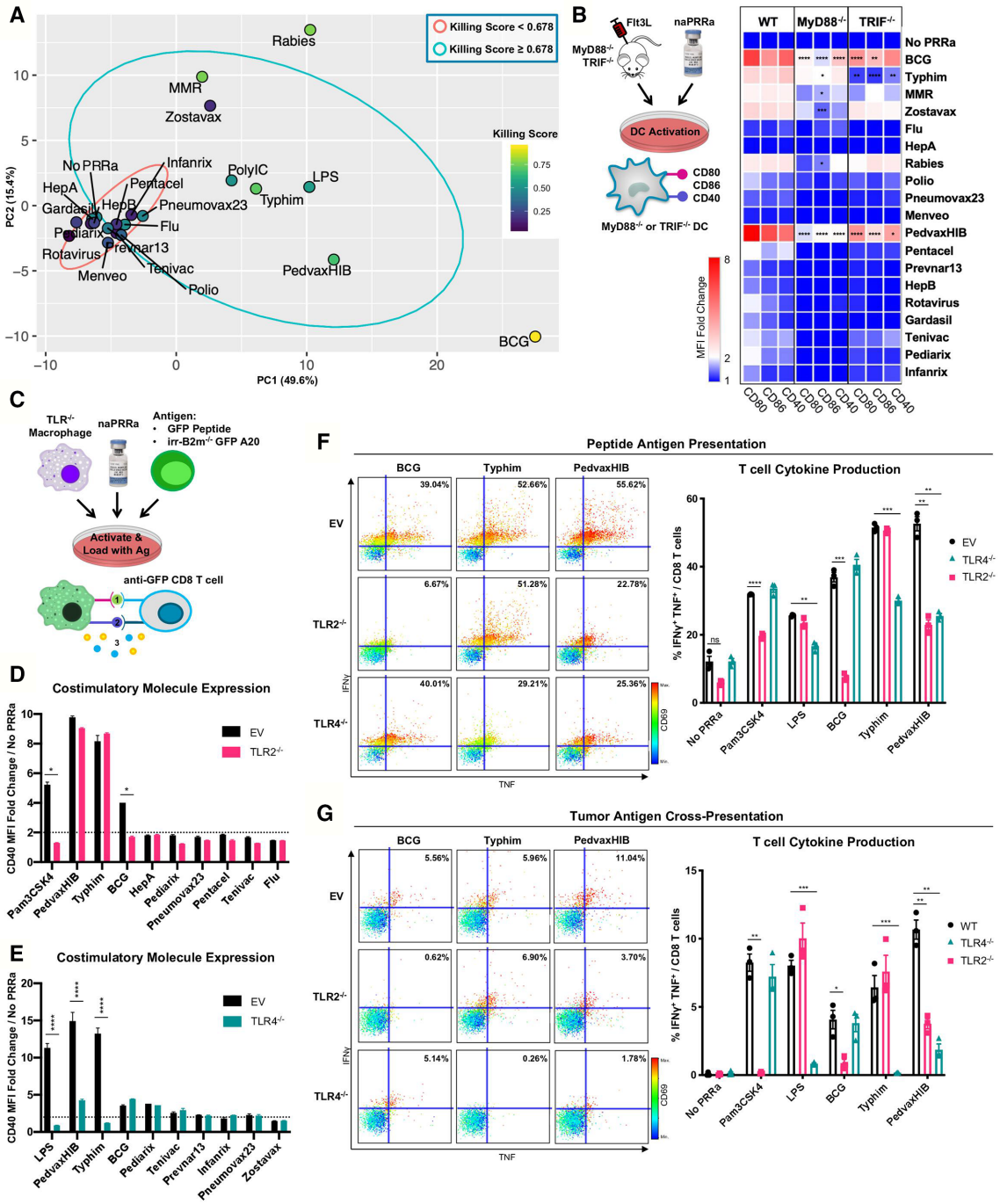

Figure 3 Individual naPRRa possess unique activation profiles and function through distinct immunological mechanisms. (A) PCA was performed with 155 phenotypic markers on murine immune cells activated with naPRRa as loading variables. Graph of PC1 and PC2 is shown. naPRRa are shaded based on potency of cytotoxic T-cell response (Killing Score). Ellipses are drawn representing naPRRa that induce significantly stronger T-cell cytotoxicity than the No PRRa condition (blue) versus naPRRa that are not superior in cytotoxic T-cell induction compared with the No PRRa condition. (B) DC activation assay using TRIF$^{-/-}$ and MyD88$^{-/-}$ mice. MyD88$^{-/-}$ DCs become less activated with Rabies, Zostavax, and MRR. BCG, Typhim, and PedvaxHIB-mediated activation is suppressed in both TRIF$^{-/-}$ and MyD88$^{-/-}$ DCs. N=3 mice for each genotype. Statistical significance was calculated by two-way ANOVA with Dunnett's multiple comparison test, comparing to wild type (WT) DCs. (c) Schema of the TLR$^{-/-}$ RAW cell activation and cross-priming assays. WT and TLR$^{-/-}$ RAW cells were activated with vaccine naPRRa, and flow cytometry was used to compare CD40 upregulation in WT vs TLR2$^{-/-}$ (D) and TLR4$^{-/-}$ (E). Statistical significance was calculated by t test. (F,G) TLR$^{-/-}$ RAW cells were cocultured with GFP peptide or XRT B2m$^{-/-}$ GFP-A20 to acquire antigen, activated with naPRRa, then cocultured with purified anti-GFP CD8 T-cells. Priming and cross-priming was measured as CD8 T-cell activation by flow cytometry. Representative scatter plots showing that naPRRa promote anti-GFP CD8 T-cell peptide antigen priming (F) or cross-priming with tumor-derived antigen (G) by targeting TLR2 and TLR4 on RAW cells. Statistical significance was calculated by t test. ANOVA, analysis of variance; DC, dendritic cells; PCA, principal component analysis; PRRa, pattern recognition receptor agonists.

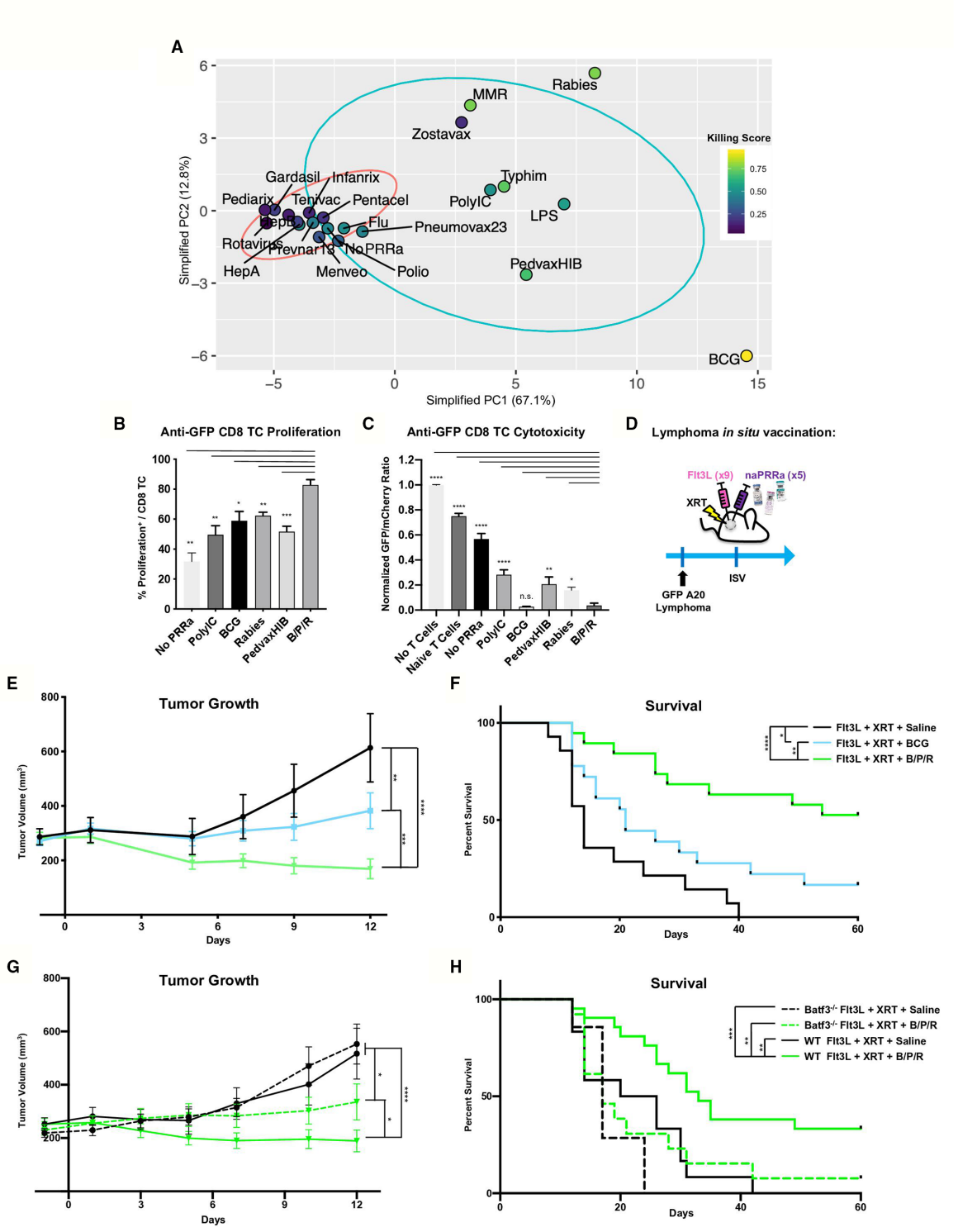

Figure 4 Rational naPRRa combinations are superior to single agent vaccines in vivo and partially dependent on Batf3 DC. (A) PCA was performed using only phenotypic markers that significantly correlated with T-cell cytotoxicity identified in online supplemental figure 6a. (B,C) Cross-presentation assay was performed, comparing the B/P/R combination versus individual naPRRa and synthetic PRRa. Statistical significance was calculated by one-way ANOVA with Dunnett's multiple comparison test. (d) Schema of murine preclinical lymphoma ISV model. GFP-A20 lymphoma-bearing mice were treated intratumorally with Flt3L. Tumors were then locally XRT, and naPRRa or saline was injected intratumorally. Mice were monitored for tumor growth (E) and survival (F). Data pooled from three independent experiments, n=20–25 mice per group. Statistical significance was calculated by two-way ANOVA with Tukey's multiple comparison test. (G,H) Murine preclinical lymphoma ISV model was performed with WT vs Batf3$^{-/-}$ mice. Animals were monitored for tumor growth (G) and survival (H). Statistical significance was calculated by two-way ANOVA with Tukey's multiple comparison test. Data pooled from two independent experiments, n=10–20 mice per group. ANOVA, analysis of variance; DC, dendritic cells; ISV, in situ vaccination; PCA, principal component analysis; PRRa, pattern recognition receptor agonists.

and online supplemental figure S6b,c). An equation was generated whereby the 43 markers are projected to a lower dimensionality space by PCA to predict cytotoxicity by placement on PC1 (online supplemental figure S6d). The cut-off for efficacy was set at the Pneumovax23 naPRRa; those to the right of Pneumovax23 on PC1 are predicted to be effective in activating DC to cross-prime CD8 T-cells in our system.

The mechanistically diverse triplet B/P/R is superior to individual naPRRa

We hypothesized that combining mechanistically distinct naPRRa would ligate diverse PRRs and optimally activate APC to potentiate T-cell priming. We resolved three distinct clusters from the PCA (figure 4A), consisting of: 1) *viral-cluster*, segregated as $PC1^{mid}/PC2^{high}$ e.g. MMR, Rabies, and Zostavax, 2) *TRIF-cluster*, segregated as $PC1^{mid}/PC2^{mid}$ for example, Typhim, PedvaxHIB (as well as PolyIC and LPS), and 3) *BCG-cluster*, segregated as $PC1^{high}/PC2^{low}$. We chose one from each cluster, selecting naPRRa that induce a unique profile of activation markers. Rabies was chosen from the viral cluster, as it was the most potent in promoting T-cell cytotoxicity after BCG. From the TRIF cluster, PedvaxHIB was chosen as it was the most potent activator of murine DC after BCG (and the most potent activator of human DC).

We first assessed the combination of BCG, PedvaxHIB, and Rabies (B/P/R) effects on DC cross-presentation in vitro. Here (and in subsequent in vivo assays), B/P/R was administered as one-third *dose of each* of the vaccines versus one *full* dose of single vaccines. B/P/R effectively promoted cross-priming, inducing greater CD8 T-cell *proliferation* than any individual naPRRa or PolyIC (figure 4B). Additionally, B/P/R-activated DC cross-prime more potent *cytotoxic* T-cells than most naPRRa or PolyIC (figure 4C). Using an ISV model similar to that in clinical trials (NCT01976585, NCT03789097), we assessed the antitumor efficacy of Flt3L, XRT, and naPRRa in vivo (figure 4D). The B/P/R combination was compared with individual BCG, given its in vitro potency and clinical use in bladder cancer and other tumors.[42 43] While BCG-ISV yielded improved tumor control compared with Flt3L and XRT alone, B/P/R-ISV was superior to BCG-ISV in inducing tumor regressions (figure 4E) and prolonging survival (figure 4F). We additionally assessed the naPRRa-ISV in the radiotherapy-resistant 4T1 breast cancer model[44] and observed that B/P/R-ISV significantly inhibited 4T1 tumor growth in vivo (online supplemental figure S7a,b).

A consideration for naPRRa clinical translation is that patients may have previously received these vaccines and have pre-existing adaptive immunity against components therein. To model potential effects of this, mice were administered B/P/R twice *prior to* tumor inoculation, as described previously[45 46] and ISV was subsequently performed (online supplemental figure S7c). We found that prior B/P/R exposure potentiated antitumor effects of naPRRa-ISV, inhibiting tumor growth (online supplemental figure S7d). These results suggest that naPRRa-ISV may be facilitated by adaptive responses to B/P/R antigens, for example, Ag85-specific[47] T-cell activation at the ISV site driving secretion of chemokines or cytokines which facilitate antitumor T-cell recruitment or priming.

Lymphoma tumor control mediated by naPRRa-ISV is partially dependent on *Batf3* DC

As BCG, PedvaxHIB, and Rabies activate multiple APC subsets in vitro, we hypothesized that the same may occur in vivo and assessed if B/P/R-ISV antitumor immunity could be generated in the absence of *Batf3* DCs. GFP-A20-bearing $Batf3^{-/-}$ and WT mice were treated with ISV with B/P/R or without PRRa. As previously, B/P/R-ISV markedly inhibited tumor growth and prolonged survival in WT mice compared with ISV without PRRa (Flt3L/XRT) (figure 4G,H). However, while tumor control by B/P/R-ISV decreased in $Batf3^{-/-}$ mice, it was still more effective than the no PRRa cohort (figure 4G, dashed green vs black curves). These results suggest that—in contrast to our previously described PolyIC-ISV[6]—naPRRa-ISV is only *partly Batf3* cDC1-dependent, suggesting that it may mediate antitumor effects via additional mechanisms, possibly through BCG, PedvaxHIB, and Rabies naPRRa-mediated activation of additional DC subsets as previously demonstrated in vitro (figure 1).

B/P/R-ISV is superior to BCG-ISV in recruitment and priming of TA-specific T-cells

To better understand B/P/R-ISV immunomodulatory effects, we examined T-cells in tumors and tumor draining lymph nodes (TdLN) of treated mice (figure 5A). Fluorescence microscopy revealed that while BCG-ISV did increase CD8 T-cell infiltration, treatment with B/P/R-ISV induced significantly greater CD8 T-cell recruitment to tumor sites (figure 5B,C). In TdLN, sites of T-cell cross-priming,[3 48] GFP-specific CD8 T effector memory ($CD44^{hi}$ $CD62L^{low}$) cells (T_{EM}) were more abundant in B/P/R-ISV treated than in BCG-ISV treated mice (figure 5D). CD8 T_{EM} in TdLN of B/P/R-ISV treated animals were more activated and proliferative, per expression of CD25, PD-1, and Ki67 (figure 5E). Intratumoral CD8 T_{EM} of B/P/R-ISV mice showed enhanced production of the critical effector molecules IFNγ and granzyme B (figure 5F). Together, these results indicate that ISV therapy with the B/P/R combination is superior in promoting T-cell mediated adaptive antitumor immunity versus single agent BCG.

B/P/R- ISV primes neoantigen-specific CD8 T-cells in vivo

Observing that ISV therapy with the naPRRa B/P/R combination potently primes model-antigen (GFP)-specific CD8 T-cells in vivo, we asked whether this approach could prime neoantigen specific T-cells. Whole exome and RNA sequencing of A20 cells was performed followed by MHC-affinity prediction and synthesis of 82 candidate neoantigen peptides, using described pipelines.[49] For each candidate, peptide-pulsed DC were cocultured with

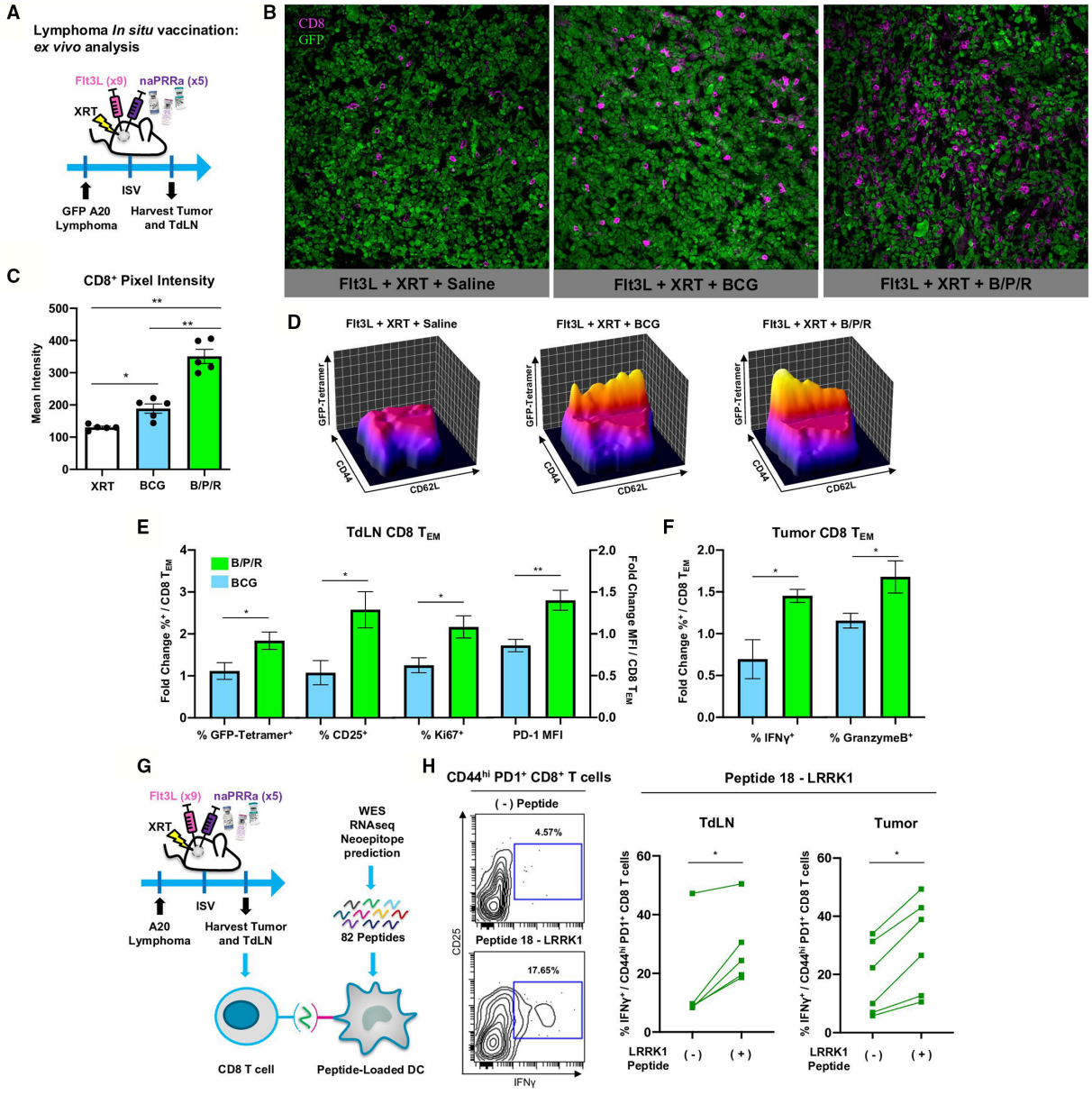

Figure 5 B/P/R-ISV is superior to ISV with single agent BCG naPRRa, promoting priming and recruitment of TA-specific T-cells. (A) Schema of murine preclinical lymphoma ISV model for ex vivo analysis. GFP-A20 lymphoma tumors were inoculated in the right flank, and tumor-bearing mice were treated intratumorally with Flt3L. Tumors were then locally irradiated (XRT), and B/P/R or saline was injected intratumorally. Mice were sacrificed on day 11 post-ISV and tumors and TdLN were harvested. (B,C) Tumors were used for analysis by fluorescence microscopy, images were analyzed and CD8 pixel intensity quantified using Fiji ImageJ software. (D–F) Tumors and TdLN were processed and analyzed by spectral flow cytometry. Statistical significance was calculated by t test. n=4–5 mice per group. (G) Schema of murine preclinical lymphoma ISV model for ex vivo T-cell neoantigen reactivity analysis. Tumor and TdLN cell suspensions isolated from tumor-bearing naPRRa-ISV treated animals were cocultured with mutant Lrrk1 peptide-pulsed DCs. T-cells were analyzed by flow cytometry after 24 hours. (H) Contour and before-after plots showing IFN-γ production by CD44⁺ PD1⁺ CD8+ T-cells. Statistical significance was calculated by t test. n=6 mice. DC, dendritic cells; ISV, in situ vaccination.

tumor and TdLN cells from B/P/R-ISV treated mice to assess T-cell neoantigen-reactivity (figure 5G). Memory ($CD44^{hi}$) CD8 T-cells reacted specifically to a 9-mer peptide for mutated LRRK1 (figure 5H), a gene implicated in B-cell proliferation.[50] This result illustrates that using commonly available off-the-shelf pathogen vaccines, B/P/R-ISV effectively primes neoantigen-specific CD8 T-cells in vivo, accomplishing the same result while saving critical time and resources compared with personalized vaccine-production strategies.

DISCUSSION

Herein, we report the most extensive immune profiling of pathogen vaccines performed to date and evidence in multiple murine and human systems to support

repurposing these as immunotherapeutic adjuvants. Previous studies using influenza vaccine as an adjuvant suggested possible DC activation.[16] A seminal study of in vitro generated monocyte-derived DCs (moDC) observed activation by pathogen vaccines,[17] though recent data demonstrate disparities between moDC and cDC1,[51] the latter being critical for cross-priming of TA-specific T-cells.[2 3 6 48] Here, we show that naPRRa differentially activate multiple APC subsets including DC, and the first data explicitly assessing TA cross-presentation.[16 17 52] The naPRRa contained in BCG, Rabies, MMR, Typhim, and PedvaxHIB promote DC cross-presentation and cross-prime CD8 T-cells, some more so than synthetic TLRa for example, PolyIC.

Interrogating naPRRa mechanisms revealed unique profiles of naPRRa and specific TLRs and pathways engaged. While TLR engagement has been described for BCG and PedvaxHIB, specific PRR are unknown for other vaccines.[14] Components of BCG can activate TLR2/TLR4,[53] TLR9,[54] NLR NOD2,[55] and some BCG-induced immune effects are MyD88-dependent,[56] supporting our findings that BCG uses *both* TRIF and MyD88-dependent pathways, but predominantly TLR2. PedvaxHIB contains *H. influenzae* b capsular polysaccharides bound to *Nisseria* outer membrane porin complex (OMPC) which include TLR2-activating porin proteins.[57] However, our observations that PedvaxHIB activates TRIF and TLR4 pathways are novel. We identify MyD88 dependence for three viral vaccines: MMR, Rabies, and Zostavax. Although measles virus is known to activate TLR2, the attenuated strain in MMR vaccine cannot.[58] Similarly, TLR7 activation has been described for Rabies virus,[59] suggesting that this vaccine *may* ligate TLR7, explaining MyD88-dependence. VZV activates human pDCs by both TLR9-dependent and TLR9-independent mechanisms[60] aligning with our observed MyD88-dependence of Zostavax. TLR4-signaling and Myd88-signaling have been described for *Salmonella* Typhi[61] and Vi capsular polysaccharides.[62] Although Typhim Vi vaccine signaling mechanisms were unknown,[17] we demonstrate its dependence on both MyD88 and TRIF as well as TLR4. While we were able to identify specific PRR mechanisms for some naPRRa, we cannot rule out that vaccine naPRRa may function through PRR mechanisms beyond TLRs. Further mechanistic studies are needed to determine if vaccine naPRRa activate STING, NLR, RLR, or additional pathways.

Using PCA, we identified 43 'simple' DC activation metrics (figure 1) that correlate with tumor cell killing in the complex T-cell killing assay (figure 2); these easily assessable metrics could be superior screening tools to better identify DC activators versus common metrics such as CD40/80/86 which would *incorrectly* predict that Zostavax might effectively activate DC to cross-prime CD8 T-cells and that MMR would not (figure 1B, figure 2F). Our agnostic approach identified unexpected cross-priming correlates, for example, lymphocytes/macrophage activation (online supplemental figure S6a) suggesting that, rather than targeting cDC1 exclusively, increasing crosstalk of multiple immune cell types, for example, macrophage activation with MMR (online supplemental figure S1b) and pDC activation with Rabies vaccines (online supplemental figure S1e), may lead to optimal cDC1-mediated cross-priming of antitumor T-cells.

Combining mechanistically distinct naPRRa yielded greater-than-additive cross-priming. This is consistent with studies showing that TRIF-activation, MyD88-activation, and multi-TLR-activation improve antipathogen[63 64] and antitumor[65 66] immunity, although caution is need when interpreting the direct link between molecular mechanism and immune effects as individual naPRRa contain unique concentrations of pathogen features. We identify that the BCG-PedvaxHIB-Rabies combination induces superior CD8 T-cell cross-priming than PolyIC, a gold-standard cDC1-activator (figure 4B,C) and functions in an ISV similar to that in early trials (NCT01976585, NCT03789097). B/P/R-ISV increases cure rates vs higher doses of single naPRRa (figure 4E,F) and induces tumor regressions in a breast cancer model (online supplemental figure S7a,b), although further studies are needed to confirm superiority of B/P/R versus other single agent or naPRRa combinations both in murine and human systems. In contrast to synthetic PRRa, patients likely have pre-existing adaptive immunity to naPRRa components, which might potentiate efficacy, as shown with reactivation of intratumoral virus-specific T-cells after viral 'vaccination'[67] and potentiation of BCG anticancer effects after pre-exposure.[68] Likewise, we observed that B/P/R pre-exposure improves tumor regressions after B/P/R-ISV (online supplemental figure S7c,d).

These data are proof of concept that naPRRa within pathogen vaccines activate subsets of murine and human APCs, including cDC1, inducing cross-priming of antitumor CD8 T-cells. Advantages of naPRRa include their regulatory-approval status, allowing for rapid translation and use as highly accessible immunomodulators for ISV or other immunotherapies. The ISV approach primes neoantigen-specific T-cells in vivo, without need for DNA/RNA sequencing, neoantigen identification, and peptide production—shortening time to therapy and reducing resource restrictions of personalized cancer vaccines.

MATERIALS AND METHODS

Ethical Compliance

Protocols for the treatment of patients, collection of human samples, and analysis were approved by the Mount Sinai Institutional Review Board under GCO-13–1347. In accordance with the Declaration of Helsinki, written informed consent was obtained from patients. Experiments were performed in compliance with relevant ethical regulations.

Animal use

All experiments were approved by the Institutional Animal Care and Use Committee of the Icahn School of

Medicine under protocol 2017–0146. Balb/c, C57BL/6, and Balb/c-Batf3$^{-/-}$ were purchased from the Jackson Laboratory and housed at the Icahn School of Medicine Animal Facility. C57BL/6 OT-I mice were a gift from Miriam Merad (Mount Sinai). JEDI mice[39] were provided by Brian D. Brown (Mount Sinai) and backcrossed on the Balb/c background for eight generations. C57BL/6-MyD88$^{-/-}$ mice were a gift from Huabao Xiong (Mount Sinai), and C57BL/6-TRIF$^{-/-}$ mice were provided by Adrian Ting (Mayo Clinic).

Patient DC activation and SEB assays

Pre-Flt3L-treatment and post-Flt3L-treatment PBMCs from four patients enrolled in ISV clinical trial NCT03789097 were isolated by density gradient centrifugation (Ficoll Paque Plus, GE Healthcare). Patient Flt3L treatment consisted of nine daily intratumoral injections of 25 µg/kg rhuFLT3L/CDX-301. For DC activation, PBMCs were plated (5×10^6 cells/mL) in 96-well U-bottom plates with 5 ug/mL synthetic TLRa or 5% v/v naPRRa for 24 hours, activation was assessed by spectral flow cytometry (Cytek Aurora). For simplicity and due to their proprietary nature, we did not attempt to normalize for naPRRa concentration and formulation differences across pathogen vaccines and used each at 5% v/v, as this concentration did not affect cell viability for most naPRRa, except the Rotavirus vaccine which was used at 1%.

Alternatively, PBMCs were stained with CellTrace Violet and 5×10^5 cells were plated in 96-well U-bottom plates, with Staphylococcal enterotoxin B (SEB) at a concentration of 40 ng/mL, along with synthetic TLRa or naPRRa. After 72 hours, T-cells were analyzed by flow cytometry (Attune NxT).

In vitro murine DC activation assays

Splenocytes from Flt3L treated mice were plated at 1×10^6 cells/mL and activated for 24 hours with 5 ug/mL of synthetic TLRa or 5% v/v naPRRa (1% for Rotavirus).

JEDI cross-presentation assay

B2m$^{-/-}$A20 or B2m$^{-/-}$GFP-A20 were resuspended (1×10^6 cells/mL), irradiated (30 Gy), and cultured for 24 hours in deep 96-well assay block plates (Corning) with synthetic TLRa or naPRRa. Flt3L splenocytes from Balb/c mice (1×10^6 cells/mL) were then added to the XRT A20 1:1 overnight. After an additional 24 hours activation step with synthetic TLRa or naPRRa, CellTrace Violet-stained JEDI splenocytes (containing anti-GFP CD45.1$^+$ CD8$^+$ T-cells) were added to the cocultures at 1:10 Flt3L-splenocytes:Jedi-splenocytes. After 72 or 96 hours, anti-GFP CD8$^+$ T-cell activation and proliferation was assessed by flow cytometry. Alternatively after 96 hours, 150 uL of the A20-Flt3L-splenocyte-Jedi-splenocyte cell suspension was transferred to 96-well U-bottom plates and 100 uL of GFP-A20 and mCherry-A20 (5×10^4 cells/mL each, 50:50 GFP:mCherry-A20) was added. Tumor cell killing by anti-GFP CD8$^+$ T-cells was assessed by flow cytometry after 24 hours.

In vivo tumor induction and ISV

2.5×10^6 GFP-A20 cells were injected in HBSS subcutaneously on the flank. The GFP-A20 cell line used for all in vivo experiments had undergone five iterations of in vivo selection to prevent rejection by naturally occurring anti-GFP T-cells. Tumor size was determined by caliper measurements (length×width×height). On day 9 after tumor inoculation, mice were injected with recombinant human Flt3L (30 µg; Celldex) intratumorally for nine daily injections. Mice were then stratified by tumor size and assigned to treatment groups; mice bearing tumors >500 mm^3 were excluded. Tumors were locally irradiated with 1 dose of 9 Gy at 2.88 Gy/min (RS 2000 X-ray irradiator, Rad Source), followed by five daily intratumoral injections of naPRRa or HBSS. Experiments with 4T1 followed a similar protocol with the following modifications: 5×10^5 4T1 cells were injected subcutaneously. Nine daily Flt3L injections were started on day 7 after tumor inoculation. On days 16 and 17, tumors were irradiated locally with two doses of 12 Gy, as previously described.[44]

Statistics

GraphPad Prism 9 software and R were used to generate graphs and perform statistical analyses. All bar graphs are displayed as mean with SEM. Statistical significance was calculated using t test, one-way analysis of variance (ANOVA), or two-way ANOVA with multiple comparisons tests, as indicated in figure legends. P>0.05 were considered non-significant; *p<0.05, **p<0.01, ***p<0.001, ****p<0.0001.

See online supplemental methods for more details.

Twitter Judit Svensson-Arvelund @JuditArvelund, Ranjan Upadhyay @RanjanMDPhD and Christine Carine Moussion @ChrMoussion

Acknowledgements We would like to thank the flow cytometry and microscopy core facilities and the CCMS animal facility at ISMMS. Raw264.7 macrophage cells were a gift from Dr Shu Hsia Chen. We would also like to thank the following funding sources: National Institutes of Health grant R37CA246239 (JDB), Cancer Research Institute Lloyd Old STAR Award (JDB), National Institutes of Health grant R01CA257195 (MM), National Institutes of Health grant R01CA254104 (MM), National Institutes of Health grant R33CA223947(BDB), National Institutes of Health grant R01AT011326 (BDB), Cancer Research Institute (BDB).

Contributors MA, JS-A, GP, KK, SAR, RU, DO, and SJ designed the experiments with the advice of MY, HM, CM, MM, BDB, and JDB. MA, JS-A, GP, KK, SAR, RU, DO, and SJ performed all experiments and analyzed the data with the help of CM, MM, BDB, and JDB. MA, JS-A, BDB, and JB wrote the manuscript. Guarantor: JDB.

Funding This study was funded by Cancer Research Institute Lloyd Old STAR Award, National Institutes of Health (R01AT011326, R01CA254104, R01CA257195, R33CA223947 (BDB), R37CA246239, Cancer Research Institute).

Competing interests None declared.

Patient consent for publication Not applicable.

Provenance and peer review Not commissioned; externally peer reviewed.

Data availability statement Data are available on reasonable request. All data relevant to the study are included in the article or uploaded as supplementary information.

ORCID iDs
Mark Aleynick http://orcid.org/0000-0001-6113-4182
Christine Carine Moussion http://orcid.org/0000-0002-1641-4094

REFERENCES

1 Hildner K, Edelson BT, Purtha WE, *et al*. Batf3 deficiency reveals a critical role for Cd8A+ Dendritic cells in cytotoxic T cell immunity. *Science* 2008;322:1097–100.
2 Broz ML, Binnewies M, Boldajipour B, *et al*. Dissecting the tumor myeloid compartment reveals rare activating antigen-presenting cells critical for T cell immunity. *Cancer Cell* 2014;26:638–52.
3 Salmon H, Idoyaga J, Rahman A, *et al*. Expansion and activation of Cd103(+) Dendritic cell progenitors at the tumor site enhances tumor responses to therapeutic PD-L1 and BRAF inhibition. *Immunity* 2016;44:924–38.
4 Spranger S, Dai D, Horton B, *et al*. Tumor-residing Batf3 Dendritic cells are required for Effector T cell trafficking and adoptive T cell therapy. *Cancer Cell* 2017;31:711–23.
5 Theisen DJ, Davidson JT, Briseño CG, *et al*. Wdfy4 is required for cross-presentation in response to viral and tumor antigens. *Science* 2018;362:694–9.
6 Hammerich L, Marron TU, Upadhyay R, *et al*. Systemic clinical tumor Regressions and potentiation of Pd1 blockade with in situ vaccination. *Nat Med* 2019;25:814–24.
7 Flowers CR, Fedewa SA, Chen AY, *et al*. Disparities in the early adoption of Chemoimmunotherapy for diffuse large B-cell lymphoma in the United States. *Cancer Epidemiol Biomarkers Prev* 2012;21:1520–30.
8 Haque W, Verma V, Butler EB, *et al*. Racial and socioeconomic disparities in the delivery of Immunotherapy for metastatic Melanoma in the United States. *J Immunother* 2019;42:228–35.
9 Hammerich L, Binder A, Brody JD. In situ vaccination: cancer Immunotherapy both personalized and off-the-shelf. *Mol Oncol* 2015;9:1966–81.
10 Brody JD, Ai WZ, Czerwinski DK, *et al*. In situ vaccination with a Tlr9 agonist induces systemic lymphoma regression: a phase I/II study. *J Clin Oncol* 2010;28:4324–32.
11 Kim YH, Gratzinger D, Harrison C, *et al*. In situ vaccination against Mycosis Fungoides by Intratumoral injection of a Tlr9 agonist combined with radiation: a phase 1/2 study. *Blood* 2012;119:355–63.
12 Geisse J, Caro I, Lindholm J, *et al*. Imiquimod 5% cream for the treatment of superficial basal cell carcinoma: results from two phase III, randomized, vehicle-controlled studies. *J Am Acad Dermatol* 2004;50:722–33.
13 Dietsch GN, Randall TD, Gottardo R, *et al*. Late-stage cancer patients remain highly responsive to immune activation by the selective Tlr8 agonist Motolimod (VTX-2337). *Clin Cancer Res* 2015;21:5445–52.
14 van Duin D, Medzhitov R, Shaw AC. Triggering TLR signaling in vaccination. *Trends Immunol* 2006;27:49–55.
15 Nichols AJ, Gonzalez A, Clark ES, *et al*. Combined systemic and Intratumoral administration of human Papillomavirus vaccine to treat multiple cutaneous Basaloid squamous cell Carcinomas. *JAMA Dermatol* 2018;154:927–30.
16 Newman JH, Chesson CB, Herzog NL, *et al*. Intratumoral injection of the seasonal flu shot converts Immunologically cold tumors to hot and serves as an Immunotherapy for cancer. *Proc Natl Acad Sci U S A* 2020;117:1119–28.
17 Schreibelt G, Benitez-Ribas D, Schuurhuis D, *et al*. Commonly used prophylactic vaccines as an alternative for synthetically produced TLR ligands to mature monocyte-derived Dendritic cells. *Blood* 2010;116:564–74.
18 Pettenati C, Ingersoll MA. Mechanisms of BCG Immunotherapy and its outlook for bladder cancer. *Nat Rev Urol* 2018;15:615–25.
19 Lavin Y, Kobayashi S, Leader A, *et al*. Innate immune landscape in early lung adenocarcinoma by paired single-cell analyses. *Cell* 2017;169:750–65.
20 Sharonov GV, Serebrovskaya EO, Yuzhakova DV, *et al*. B cells, plasma cells and antibody Repertoires in the tumour Microenvironment. *Nat Rev Immunol* 2020;20:294–307.
21 Curtsinger JM, Gerner MY, Lins DC, *et al*. Signal 3 availability limits the Cd8 T cell response to a solid tumor. *J Immunol* 2007;178:6752–60.
22 Haabeth OAW, Lorvik KB, Yagita H, *et al*. Interleukin-1 is required for cancer eradication mediated by tumor-specific Th1 cells. *Oncoimmunology* 2016;5:e1039763.
23 Dufour JH, Dziejman M, Liu MT, *et al*. IFN-gamma-inducible protein 10 (IP-10; Cxcl10)-Deficient mice reveal a role for IP-10 in Effector T cell generation and trafficking. *J Immunol* 2002;168:3195–204.
24 Chheda ZS, Sharma RK, Jala VR, *et al*. Chemoattractant receptors Blt1 and Cxcr3 regulate antitumor immunity by facilitating Cd8+ T cell migration into tumors. *J Immunol* 2016;197:2016–26.
25 Wendel M, Galani IE, Suri-Payer E, *et al*. Natural killer cell accumulation in tumors is dependent on IFN-gamma and Cxcr3 ligands. *Cancer Res* 2008;68:8437–45.
26 Dangaj D, Bruand M, Grimm AJ, *et al*. Cooperation between Constitutive and inducible Chemokines enables T cell Engraftment and immune attack in solid tumors. *Cancer Cell* 2019;35:885–900.
27 Allen F, Bobanga ID, Rauhe P, *et al*. Ccl3 augments tumor rejection and enhances Cd8+ T cell infiltration through NK and Cd103+ Dendritic cell recruitment via IFNγ. *Oncoimmunology [Internet]* 2017. 10.1080/2162402X.2017.1393598 Available: https://pubmed.ncbi.nlm.nih.gov/29399390/?from_single_result=%28%22Oncoimmunology%22%5BJournal%5D%29+AND+%28allen%5BAuthor+-+First%5D%29
28 Fuertes MB, Kacha AK, Kline J, *et al*. Host type I IFN signals are required for antitumor Cd8+ T cell responses through Cd8A+ Dendritic cells. *J Exp Med* 2011;208:2005–16.
29 Diamond MS, Kinder M, Matsushita H, *et al*. Type I interferon is selectively required by Dendritic cells for immune rejection of tumors. *J Exp Med* 2011;208:1989–2003.
30 Tamura T, Yanai H, Savitsky D, *et al*. The IRF family transcription factors in immunity and Oncogenesis. *Annu Rev Immunol* 2008;26:535–84.
31 Perng Y-C, Lenschow DJ. Isg15 in antiviral immunity and beyond. *Nat Rev Microbiol* 2018;16:423–39.
32 Marshall N, Hutchinson K, Marron TU, *et al*. Antitumor t-cell Homeostatic activation is Uncoupled from Homeostatic inhibition by Checkpoint blockade. *Cancer Discov* 2019;9:1520–37.
33 Whitfield SJC, Taylor C, Risdall JE, *et al*. Interference of the T cell and antigen-presenting cell Costimulatory pathway using Ctla4-IG (Abatacept) prevents Staphylococcal Enterotoxin B pathology. *J Immunol* 2017;198:3989–98.
34 Ariffin JK, Sweet MJ. Differences in the repertoire, regulation and function of toll-like receptors and Inflammasome-forming nod-like receptors between human and Mouse. *Curr Opin Microbiol* 2013;16:303–10.
35 Norbury CC, Chambers BJ, Prescott AR, *et al*. Constitutive Macropinocytosis allows TAP-dependent major Histocompatibility complex class I presentation of exogenous soluble antigen by bone marrow-derived Dendritic cells. *Eur J Immunol* 1997;27:280–8.
36 Garg AD, Elsen S, v. KD, *et al*. Resistance to anticancer vaccination effect is controlled by a cancer cell-autonomous phenotype that disrupts Immunogenic Phagocytic removal. *Oncotarget [Internet]* 2015;6:26841–60.
37 Sancho D, Joffre OP, Keller AM, *et al*. Identification of a Dendritic cell receptor that couples sensing of necrosis to immunity. *Nature* 2009;458:899–903.
38 Zhang J-G, Czabotar PE, Policheni AN, *et al*. The Dendritic cell receptor Clec9A binds damaged cells via exposed actin filaments. *Immunity* 2012;36:646–57.
39 Agudo J, Ruzo A, Park ES, *et al*. GFP-specific Cd8 T cells enable targeted cell depletion and visualization of T-cell interactions. *Nat Biotechnol* 2015;33:1287–92.
40 Upadhyay R, Boiarsky JA, Pantsulaia G, *et al*. A critical role for Fas-mediated off-target tumor killing in T-cell Immunotherapy. *Cancer Discov* 2021;11:599–613.
41 Svensson-Arvelund J, Cuadrado-Castano S, Pantsulaia G, *et al*. Expanding cross-presenting Dendritic cells enhances Oncolytic Virotherapy and is critical for long-term anti-tumor immunity. *Nature Communications* 2022;13:.:7149.
42 Marabelle A, Kohrt H, Caux C, *et al*. Intratumoral immunization: a new paradigm for cancer therapy. *Clin Cancer Res* 2014;20:1747–56.

43 Aleynick M, Svensson-Arvelund J, Flowers CR, *et al*. Pathogen molecular pattern receptor agonists: treating cancer by mimicking infection. *Clin Cancer Res* 2019;25:6283–94.
44 Demaria S, Kawashima N, Yang AM, *et al*. Immune-mediated inhibition of metastases after treatment with local radiation and CTLA-4 blockade in a mouse model of breast cancer. *Clin Cancer Res* 2005;11(2 Pt 1):728–34.
45 Cervantes-Villagrana AR, Hernández-Pando R, Biragyn A, *et al*. Prime-boost BCG vaccination with DNA vaccines based in Β-Defensin-2 and Mycobacterial antigens Esat6 or Ag85B improve protection in a tuberculosis experimental model. *Vaccine* 2013;31:676–84.
46 Xu Y, Yang E, Wang J, *et al*. Prime-boost Bacillus Calmette-Guérin vaccination with Lentivirus-Vectored and DNA-based vaccines expressing antigens Ag85B and Rv3425 improves protective efficacy against Mycobacterium tuberculosis in mice. *Immunology* 2014;143:277–86.
47 Nadia C, Serena M, Carmela La M, *et al*. Phenotypical and functional analysis of memory and Effector human Cd8 T cells specific for Mycobacterial antigens. *J Immunol* 2006.
48 Roberts EW, Broz ML, Binnewies M, *et al*. Critical role for Cd103+/Cd141+ Dendritic cells bearing Ccr7 for tumor antigen trafficking and priming of T cell immunity in Melanoma. *Cancer Cell* 2016;30:324–36.
49 Perumal D, Imai N, Laganà A, *et al*. Mutation-derived Neoantigen-specific T-cell responses in multiple myeloma. *Clin Cancer Res* 2020;26:450–64.
50 Morimoto K, Baba Y, Shinohara H, *et al*. Lrrk1 is critical in the regulation of B-cell responses and Carma1-dependent NF-ΚB activation. *Sci Rep* 2016;6.
51 Carpentier S, Vu Manh T-P, Chelbi R, *et al*. Comparative Genomics analysis of mononuclear phagocyte Subsets CONFIRMS Homology between Lymphoid tissue-resident and Dermal Xcr1+ Dcs in Mouse and human and distinguishes them from Langerhans cells. *J Immunol Methods* 2016;432:35–49.
52 Bol KF, Aarntzen EHJG, Pots JM, *et al*. Prophylactic vaccines are potent Activators of monocyte-derived Dendritic cells and drive effective anti-tumor responses in Melanoma patients at the cost of toxicity. *Cancer Immunol Immunother* 2016;65:327–39.
53 Uehori J, Fukase K, Akazawa T, *et al*. Dendritic cell maturation induced by Muramyl Dipeptide (MDP) derivatives: Monoacylated MDP confers Tlr2/Tlr4 activation. *J Immunol* 2005;174:7096–103.
54 Bafica A, Scanga CA, Feng CG, *et al*. Tlr9 regulates Th1 responses and cooperates with Tlr2 in mediating optimal resistance to Mycobacterium tuberculosis. *J Exp Med* 2005;202:1715–24.
55 Divangahi M, Mostowy S, Coulombe F, *et al*. Nod2-deficient mice have impaired resistance to Mycobacterium tuberculosis infection through defective innate and adaptive immunity. *J Immunol* 2008;181:7157–65.
56 Tanaka H, Mori Y, Ishii H, *et al*. Enhancement of metastatic capacity of fibroblast-tumor cell interaction in mice. *Cancer Res* 1988;48:1456–9.
57 Latz E, Franko J, Golenbock DT, *et al*. Haemophilus influenzae type B-outer membrane protein complex Glycoconjugate vaccine induces cytokine production by engaging human toll-like receptor 2 (Tlr2) and requires the presence of Tlr2 for optimal Immunogenicity. *J Immunol* 2004;172:2431–8.
58 Bieback K, Lien E, Klagge IM, *et al*. Hemagglutinin protein of wild-type measles virus activates toll-like receptor 2 signaling. *J Virol* 2002;76:8729–36.
59 Luo Z, Li Y, Zhou M, *et al*. Toll-like receptor 7 enhances Rabies virus-induced humoral immunity by facilitating the formation of germinal centers. *Front Immunol* 2019;10:429:429.:.
60 Yu H-R, Huang H-C, Kuo H-C, *et al*. IFN-Α production by human mononuclear cells infected with Varicella-Zoster virus through Tlr9-dependent and -Independent pathways. *Cell Mol Immunol* 2011;8:181–8.
61 Wilson RP, Raffatellu M, Chessa D, *et al*. The VI-capsule prevents toll-like receptor 4 recognition of salmonella. *Cell Microbiol* 2008;10:876–90.
62 Garg R, Akhade AS, Yadav J, *et al*. Myd88-dependent pro-inflammatory activity in VI polysaccharide vaccine against typhoid promotes AB switching to IgG. *Innate Immun* 2015;21:778–83.
63 Napolitani G, Rinaldi A, Bertoni F, *et al*. Selected toll-like receptor agonist combinations synergistically trigger a T helper type 1–polarizing program in Dendritic cells. *Nat Immunol* 2005;6:769–76.
64 Zhu Q, Egelston C, Vivekanandhan A, *et al*. Toll-like receptor ligands Synergize through distinct Dendritic cell pathways to induce T cell responses: implications for vaccines. *Proc Natl Acad Sci U S A* 2008;105:16260–5.
65 Craft N, Bruhn KW, Nguyen BD, *et al*. The Tlr7 agonist Imiquimod enhances the anti-Melanoma effects of a recombinant Listeria Monocytogenes vaccine. *J Immunol* 2005;175:1983–90.
66 Kidner TB, Morton DL, Lee DJ, *et al*. Combined Intralesional Bacille Calmette-Guérin (BCG) and topical Imiquimod for in-transit Melanoma. *J Immunother* 2012;35:716–20.
67 Rosato PC, Wijeyesinghe S, Stolley JM, *et al*. Virus-specific memory T cells populate tumors and can be Repurposed for tumor Immunotherapy. *Nat Commun* 2019;10:567.
68 Biot C, Rentsch CA, Gsponer JR, *et al*. Preexisting BCG-specific T cells improve intravesical Immunotherapy for bladder cancer. *Sci Transl Med* 2012;4:137ra72.